ARTICLE
Journal of Cellular Biochemistry 111:1179–1187 (2010)

Journal of Cellular Biochemistry

Microarray Profile of Gene Expression During Osteoclast Differentiation in Modelled Microgravity

Yuvaraj Sambandam,[1] Jeremy J. Blanchard,[1] Giffin Daughtridge,[1] Robert J. Kolb,[1] Srinivasan Shanmugarajan,[1] Subramanya N. M. Pandruvada,[1] Ted A. Bateman,[2] and Sakamuri V. Reddy[1*]

[1] *Charles P. Darby Children's Research Institute, Medical University of South Carolina, Charleston, South Carolina*
[2] *Osteoporosis Biomechanics Laboratory, Department of Bioengineering, Clemson University, Clemson, South Carolina*

ABSTRACT

Microgravity (μXg) leads to a 10–15% loss of bone mass in astronauts during space flight. Osteoclast (OCL) is the multinucleated bone-resorbing cell. In this study, we used the NASA developed ground-based rotating wall vessel bioreactor (RWV), rotary cell culture system (RCCS) to simulate μXg conditions and demonstrated a significant increase (2-fold) in osteoclastogenesis compared to normal gravity control (Xg). Gene expression profiling of RAW 264.7 OCL progenitor cells in modelled μXg by Agilent microarray analysis revealed significantly increased expression of critical molecules such as cytokines/growth factors, proteases and signalling proteins, which play an important role in enhanced OCL differentiation/function. Transcription factors such as c-Jun, MITF and CREB implicated in OCL differentiation are upregulated; however no significant change in the levels of NFATc1 expression in preosteoclast cells subjected to modelled μXg. We also identified high-level expression of calcium-binding protein, S100A8 (calcium-binding protein molecule A8/calgranulin A) in preosteoclast cells under μXg. Furthermore, modelled μXg stimulated RAW 264.7 cells showed elevated cytosolic calcium (Ca^{2+}) levels/oscillations compared to Xg cells. siRNA knock-down of S100A8 expression in RAW 264.7 cells resulted in a significant decrease in modelled μXg stimulated OCL differentiation. We also identified elevated levels of phospho-CREB in preosteoclast cells subjected to modelled μXg compared to Xg. Thus, modelled μXg regulated gene expression profiling in preosteoclast cells provide new insights into molecular mechanisms and therapeutic targets of enhanced OCL differentiation/activation to prevent bone loss and fracture risk in astronauts during space flight missions. J. Cell. Biochem. 111: 1179–1187, 2010.

KEY WORDS: OSTEOCLAST; MICROGRAVITY; MICROARRAY; ROTATING WALL VESSEL BIOREACTOR (RWV); NASA

Microgravity (μXg) or weightlessness conditions during space flight results in biological changes in astronauts, which include atrophy of the muscular system [Katkovsky and Pomyotov, 1976; Miyamoto et al., 1998], immune system dysfunction [Sonnenfeld et al., 2003] and cardiovascular anomalies [Arbeille et al., 1995; White and Blomqvist, 1998]. A primary challenge for The National Aeronautics and Space Association (NASA) is preventing accelerated bone loss and fracture risk in astronauts. In space, astronauts are exposed to μXg; 0.08–0.008*g* rather than Earths inherent gravity of 1*g*. Thus, little to no pressure is exerted on the astronaut's skeletal system. This skeleton unloading over time reduces bone mineral density (BMD), particularly in load-bearing regions of the skeleton such as the legs and lower back may leads to fracture risk in austronauts [Lang et al., 2004; Lang et al., 2006; Keyak et al., 2009]. In fact, morphological changes in bones of astronauts after space flight resemble osteoporotic patients [Garber et al., 2000; Lang et al., 2006; Keyak et al., 2009]. Furthermore, serum and urine calcium levels are elevated in astronauts throughout the space mission. During long-term space missions, astronauts can lose as much bone mass in the proximal femur in 1 month as post-menopausal women on Earth lose in 1 year [Cavanagh et al., 2005]. It has been reported that astronauts can lose 1–2% of entire bone mass per month, while in space, underscoring the hazards of current and future long-term space flight missions [Carmeliet and Bouillon, 1999]. The possibility of irreversible bone loss has serious implications for long-term inhabitants of the International Space Station. Although nutritional supplementation and regimented exercise are mandated for astronauts, bone loss is still an impending issue. Previously, isolated fetal mouse long bones under near weightless conditions showed decreased mineralization

Additional Supporting Information may be found in the online version of this article.

Grant sponsor: South Carolina EPSCoR; Grant number: NGT5-40099; Grant sponsor: EPSCoR Consortium REU.

*Correspondence to: Dr. Sakamuri V. Reddy, PhD, Charles P. Darby Children's Research Institute, 173 Ashley Avenue, Medical University of South Carolina, Charleston, SC 29425. E-mail: reddysv@musc.edu

Received 2 June 2010; Accepted 3 August 2010 • DOI 10.1002/jcb.22840 • © 2010 Wiley-Liss, Inc.
Published online 17 August 2010 in Wiley Online Library (wileyonlinelibrary.com).

and increased calcium release [Van Loon et al., 1995]. Similarly, it has been shown that osteopenia in the immobilized rat hind limb model is associated with increased bone resorption and decreased bone formation. Cell culture systems demonstrated decreased osteoblastic activity under μXg conditions [Van Loon et al., 1995; Hughes-Fulford and Lewis, 1996].

The osteoclast (OCL) is the bone-resorbing cell derived from monocyte/macrophage lineage. The TNF family member, receptor activator for nuclear factor κ B ligand (RANKL) is expressed in marrow stromal/osteoblast cells in response to several osteotropic factors and is critical for OCL precursor differentiation to form multinucleated OCL, which resorb bone. M-CSF is required for proliferation and survival of OCL precursors. The interaction of RANKL and RANK expressed on preosteoclast cells results in activation of various signalling cascades during OCL differentiation and bone resorption [Reddy, 2004]. Evidence suggests that μXg modulates RANKL and osteoprotegerin (OPG) gene expression in bone marrow stromal/preosteoblast cells, which are key regulators of osteoclastogenesis and bone resorption [Kanematsu et al., 2002; Rucci et al., 2007]. It has also been shown that hypergravity has no effect on the number of OCLs, but enhances bone-resorption activity [Nemoto and Uemura, 2000]. Recently, μXg has been reported to reduce osteoblast life-span and enhance IL-6 gene expression, thereby decreasing osteoblast activity and increasing OCL activity to contribute to bone loss associated with weightlessness [Rucci et al., 2002]. Furthermore, intact limb bones of newts flown onboard the biosatellite Cosmos-2229 had increased calcium and histological analysis revealed activation of osteoclastic resorption on the endosteal surface of long bones on the 20th day of space flight [Berezovska et al., 1998]. Thus, increased OCL activity has been reported under μXg conditions. μXg perturbs bone remodelling by uncoupling bone formation and bone resorption which could account for bone loss [Nichols et al., 2006]. However, the mechanism underlying μXg-induced OCL formation/bone resorption activity is unclear. In this study, we used the NASA developed ground-based rotating wall vessel bioreactor (RWV), rotary cell culture system (RCCS) to simulate μXg conditions and demonstrated a significant increase in osteoclastogenesis in mouse bone marrow cultures. We further determined the gene expression profiling during OCL differentiation of RAW 264.7 cells subjected to modelled μXg by Agilent chip microarray analysis.

METHODS

MODELLED μXg AND CELL CULTURE

The RWV, RCCS (Synthecon Inc, TX) is a horizontally rotated, bubble-free cell culture vessel with a silicone membrane for gas exchange. The fluid dynamic principles of the RCCS allow oxygenation without turbulence, co-localization of particles with different sedimentation rates and reduction of fluid shear forces [Goodwin et al., 1993; Zayzafoon et al., 2004]. Suspension of cells established a uniform, very low shear, three-dimensional (3D) spatial freedom and fluid suspension orbit within the cell culture vessel. The vessel containing mouse bone marrow-derived non-adherent cells or RAW 264.7 cells suspended in α-MEM containing 10% foetal bovine serum (FBS) was rotated at 16 rpm for 24 h to simulate a μXg (0.008*g*) environment, termed as modelled μXg, in a humidified incubator at 37°C with 5% CO_2. Cells cultured under normal gravity conditions termed as control (Xg).

OSTEOCLAST CULTURE

Bone marrow was flushed from long bones of 6- to 8-week-old mice (C57BL/6) using α-MEM. Cells were pelleted at 1,500 rpm for 7 min at room temperature and plated in α-MEM with 10% FBS supplemented with M-CSF (10 ng/ml) and cultured overnight. Non-adherent mouse bone marrow cells (1.5×10^6/ml) or RAW 264.7 cells (1×10^4/ml) subjected to modelled μXg in RCCS for 24 h were cultured in a 24-well plate for 7 or 5 days, respectively, in the presence of M-CSF (10 ng/ml) and RANKL (80 ng/ml; R&D Systems Inc., Minneapolis, MN). Cells were fixed with 2% glutaraldehyde in phosphate-buffered saline (PBS) and stained for tartrate-resistant acid phosphatase (TRAP) activity using a histochemical kit (Sigma Chemical Co., St. Louis, MO). TRAP-positive multinucleated cells (MNC) containing three or more nuclei were scored as OCLs under a microscope as described [Shanmugarajan et al., 2007].

siRNA INTERFERENCE

RAW 264.7 cells were seeded (5×10^5 cells/well) in six-well plates and supplemented with DMEM containing 10% FBS. One day after seeding, cells were transfected with double-stranded-specific siRNA (10 μmol/L) against S100A8 (Santa Cruz Biotechnology, Inc., CA) by oligofectamine as per the manufacturer instructions (Invitrogen Life Technologies, Inc., Carlsbad, CA). Non-specific scrambled siRNA-transfected cells served as control. Cells were cultured in modelled μXg for 24 h and both Xg and μXg subjected cells were cultured in the presence of M-CSF (10 ng/ml) and RANKL (80 ng/ml) for 5 days to form OCLs.

MICROARRAY ANALYSIS

RAW 264.7 cells (1.5×10^6/ml) were subjected to RCCS with DMEM containing 10% FBS for 24 h and stimulated with RANKL (80 ng/ml) for 24 h in parallel with Xg cells. Total RNA isolated using RNAzol reagent (Biotecx Labs, Houston, TX) was hybridized with Agilent whole genome 4 K × 44 K array system (~26,000 genes). Slides were washed and scanned by using an Agilent G2565 microarray scanner. Data obtained were analyzed with Agilent feature extraction and GeneSpring GX v7.3.1 software packages (Genus Biosystem, Inc. Northbrook, IL). Gene Ontology Tree Machine (GOTM) is a web-based platform used for interpreting gene sets including microarray data using Gene Ontology hierarchies [Zhang et al., 2004] The GOTM provides classification and distribution of genes as well as analytical tools for comparison of the significantly enriched gene numbers in the catalogue of gene ontology in a pathway or gene family oriented way for differential gene expression with a reference gene set, which includes all the genes in the mouse genome. The hypergeometric test, which is appropriate for sampling without replacement, was adopted by GOTM to determine whether those enrichments are statistically significant.

QUANTITATIVE REAL-TIME RT-PCR

Total RNA was isolated from mouse bone marrow-derived non-adherent cells subjected to modelled μXg or Xg conditions were

treated with or without of M-CSF (10 ng/ml) and RANKL (80 ng/ml) for 24 h using RNAzol reagent (Biotecx Labs). The reverse transcription reaction was performed using poly-dT primer and Moloney murine leukemia virus reverse transcriptase (Applied Biosystems, Foster City, CA) in a 25 μl reaction volume containing total RNA (2 μg), 1× PCR buffer and 2 mM $MgCl_2$, at 42°C for 15 min followed by 95°C for 5 min. The quantitative real-time PCR was performed using IQ™ SYBR Green Supermix in an iCycler (iCycler iQ Single-color Real-Time PCR detection system; Bio-Rad, Hercules, CA). The forward and reverse primer sequences used to amplify the selected genes are listed as follow:

Primer	Forward (5'–3')	Reverse (5'–3')
Cathepsin-L	GCTTGGGAACAGCCTTAG	GTTGCTGTATTCCCCGTTGT
Cathepsin-B	TGAAGAAGCTGTGTGGCACT	GTTCGGTCAGAAATGGCTTC
Cathepsin-K	CTCTCGGCGTTTAATTTGGG	GCTAAATGCAGAGGGTACAGAG
MMP-8	AGGGCTGAAGTGAAAACAGC	ATTCCATTGGGTCCATCAAA
MMP-12	TGAAAGGAGTCTGCACAATGA	CAGAGTTGAGTTGTCCAGTTGC
MMP-13	ATCCTGGCCACCTTCTTCTT	TTTCTCGGAGCCTGTCAACT
CAR-4	CCTGGAGCCTGTAAGGAGAA	AGCGTCATCTCCACTGTGTG
ATPase	AGCTTGGGAAGGTCCAATTT	GGTTTTCACCGGTGTCCATA
S100A8	GAGAAGGCCTTGAGCAACC	TGACCATTTTCTTGAAGTCATTC
c-Jun	TGACTGCAAAGATGGAAACG	GAGGTGCGGCTTCAGACT
MITF	AGGGAGCAGCAGCAGAAG	AGGACTTGGCTGGCATGTT
GAPDH	CCTACCCCCAATGTATC CGTTGTG	GGAGGAATGGGAGTTGCTG TTGAA

Thermal cycling parameters were 94°C for 3 min, followed by 40 cycles of amplifications at 94°C for 30 s, 60°C for 1 min, 72°C for 1 min and 72°C for 5 min as the final elongation step. Relative levels of mRNA expression were normalized in all the samples analyzed with respect to the levels of GAPDH amplification as described [Bustin, 2000].

WESTERN BLOT ANALYSIS

Mouse bone marrow-derived non-adherent cells or RAW 264.7 cells supplemented with α-MEM containing 10% FBS were subjected to modelled μXg. Cells were stimulated with or without RANKL (80 ng/ml) in the presence of M-CSF (10 ng/ml) for 24 h and total cell lysates were prepared in a buffer containing 20 mM Tris–HCl at pH 7.4, 1% Triton X-100, 1 mM EDTA, 1.5 mM $MgCl_2$;10% glycerol, 150 mM NaCl, 0.1 mM Na_3VO_4 and 1× protease inhibitor cocktail. The protein content of the samples was measured using the BCA protein assay reagent (Pierce, Rockford, IL). Protein (100 μg) samples were then subjected to SDS–PAGE using 4–15% Tris–HCl gradient gels and blot transferred on to a PVDF membrane, immunoblotted with anti-cathepsin K (Ctsk), anti-S100A8, anti-NFATc1 (Santa Cruz Biotechnology Inc., CA) and anti-phospho-CREB (R&D Systems Inc.) antibodies. The bands were detected using the enhanced chemiluminescence detection system (Pierce). The band intensity was quantified by densitometric analysis using the NIH ImageJ Program.

Ca^{2+} MEASUREMENTS

RAW 264.7 cells subjected to modelled μXg or Xg were incubated with RANKL (80 ng/ml) for 24 h and then with 4.6 μM fluo-4 AM and 14 μM Fura Red AM and 0.05% pluronic F127 for 30 min. Cells were rinsed 3× with Ringers solution and then equilibrated in serum-free IMDM medium without Phenol Red and stimulated with RANKL (80 ng/ml) for 20 min. Calcium (Ca^{2+}) levels/oscillations were analyzed by live cell confocal microscopy (Leica Microsystems, Heidelberg, Germany) and fluorescence was continuously recorded at 520 and 600 nm emission. The ratio of fluorescence intensity of Fluo-4 to Fura Red was calculated to estimate relative changes in cytosolic Ca^{2+} levels as described [Takayanagi et al., 2002a].

STATISTICAL ANALYSIS

Results are presented as mean ± SD for three independent experiments and were compared using the Student's *t*-test. Results were considered significantly different for $P < 0.05$. Pearson's correlation coefficient (R^2) was calculated using Microsoft Excel 2000 software.

RESULTS

μXg MODULATION OF OCLs FORMATION

μXg associated with space flight is a challenge for normal bone homeostasis. To determine the effect of simulated μXg on OCL differentiation in vitro, mouse bone marrow-derived non-adherent cells were subjected to modelled μXg in the RCCS as described in Methods Section. After 24 h both Xg and μXg subjected cells were stimulated with M-CSF (10 ng/ml) and RANKL (80 ng/ml) for 7 days to form multinucleated OCLs. As shown in Figure 1A,B, modelled

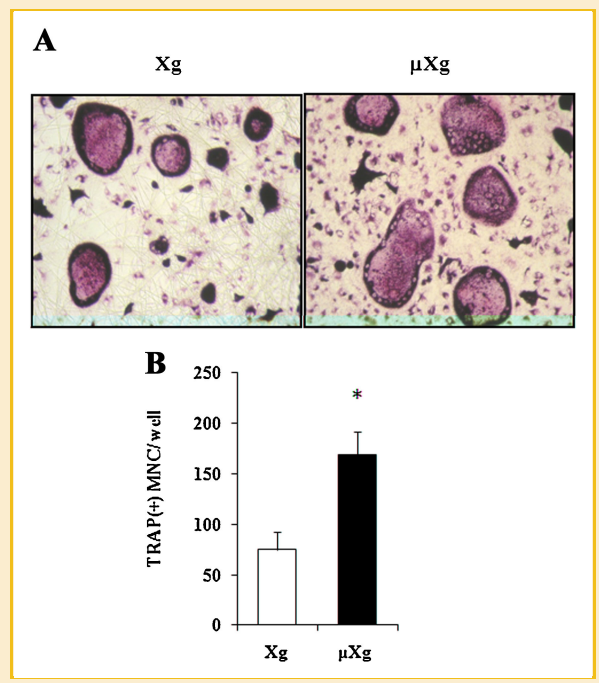

Fig. 1. Microgravity (μXg) modulation of osteoclastogenesis. A: Mouse bone marrow-derived non-adherent cells were either subjected to modelled μXg for 24 h or control (Xg) and cultured with M-CSF (10 ng/ml) and RANKL (80 ng/ml) for 7 days to form OCLs. Cells were fixed and stained for TRAP activity. Photomicrographs were taken at magnification ×20. B: TRAP-positive multinucleated cells (MNC) containing three or more nuclei were scored as OCL. The results represent quadruplicate cultures of three independent experiments (*$P < 0.05$). [Color figure can be viewed in the online issue, which is available at wileyonlinelibrary.com]

μXg resulted in a significant increase in number and size of TRAP-positive multinucleated OCL formation compared to Xg cultures. These results are consistent with the recent findings in a space flight (FOTON-M3 mission) that μXg modulates osteoclastogenesis [Tamma et al., 2009].

GENE EXPRESSION PROFILE OF PREOSTEOCLASTS IN MODELLED μXg

To assess the gene expression pattern of preosteoclasts under μXg, we performed large-scale gene expression profiling using the Agilent whole genome 4 K × 44 K array system which analyzes ~26,000 genes. We subjected a homogeneous population of RAW 264.7 OCL progenitor cells to modelled μXg in RCCS for 24 h and stimulated with RANKL (80 μg/ml) for 24 h. Agilent chips were hybridized with total RNA isolated from Xg and μXg subjected RAW 264.7 cells. Gene array data were analyzed using stringent criteria that restricted the scored genes for specific hybridization values ≥2-fold. Thus, 3,404 genes were identified that are differentially expressed in preosteoclast cells under μXg conditions. Scatter plot and functional gene cluster analysis revealed differential gene expression in modelled μXg compared to static Xg (Fig. 2A,B). Microarray profiling of modelled μXg regulated gene expression in RAW 264.7 preosteoclast cells was deposited in Gene Expression Omnibus (GEO) database repository at NCBI (Accession #GSE21093). Gene expression profiles were analyzed by GOTM, a web-based platform and modelled μXg-induced genes were functionally grouped for cytokines/growth factors, chemokines, signalling/interacting proteins, adhesion and trafficking proteins, proteases, calcium signalling and ATPases genes (Supplemental Tables I–VII). Thus, 11.4% of the genes analyzed were differentially regulated by μXg; of these 54% were upregulated and 45% were downregulated. Several genes important for osteoclastogenesis and bone resorption function were elevated in modelled μXg compared to Xg. Specifically, μXg upregulated mRNA expression of colony stimulating factor 3 (granulocyte; csf3, 16-fold), Fc receptor2b (Fcgr2b, 7-fold), integrin αV (Itgav, 3-fold), bone matrix degrading proteases (matrix metalloproteinase) MMP-8 (30-fold), MMP-12 (10-fold), MMP-13 (7-fold), cathepsin B (Ctsb, 3.5-fold), cathepsin L (Ctsl, 2.4-fold), Ctsk (2.3-fold), ATPase, H^+ transporting lysosomal (Atp6v0a1, 3.5-fold), chloride channel calcium activated 1 (Clca1, 3.8-fold), transcription factors, c-Jun (2-fold) MITF (2.2-fold), c-AMP responsive element-binding proteins (CREBs, 2.2- to 3.4-fold), vesicular secretion factors, carboxypeptidase E (Cpe, 14-fold) and ATP-binding cassette C (Abcc3, 10-fold). Furthermore, μXg elevated gene expression of adhesion molecules such as podoplanin (Pdpn, 138-fold), integrin β7 (Itgb7, 11.8-fold), integrin β5 (Itgb5, 6.2-fold), integrin αM (Itgam, 4-fold), integrin β4 (Itgb4,

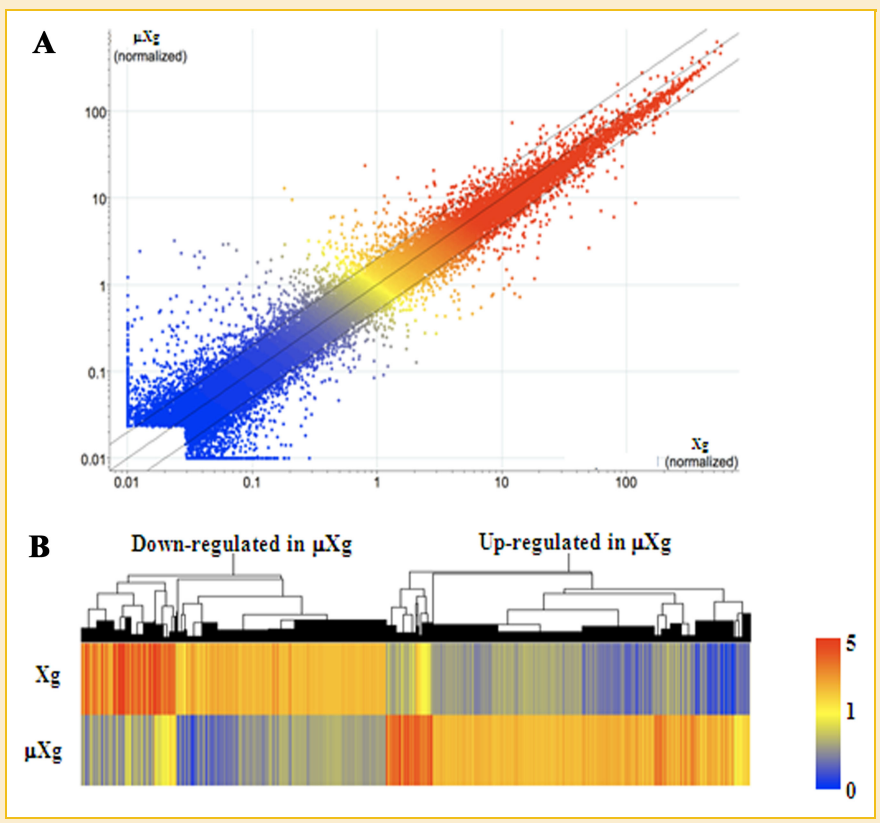

Fig. 2. Microarray profiling of gene expression in RAW 264.7 cells under μXg. RAW 264.7 cells were cultured in modelled μXg for 24 h and stimulated with RANKL (80 ng/ml) for 24 h. Preosteoclast cultures under normal gravity (Xg) served as control cells. Total RNA isolated from the cells was subjected to Agilent whole genome 4 K × 44 K array system for microarray analysis. (A) Scatter plot and (B) Cluster analysis of ~26,000 genes revealed differential gene expression in modelled μXg. Gene expression profile presented as: Red—high expression; Yellow—medium expression; Blue—low expression. Pearson's correlation coefficient ($R^2 = 0.53$) for Scatter plot was calculated. [Color figure can be viewed in the online issue, which is available at wileyonlinelibrary.com]

3.3-fold), integrin αL (Itgal, 2.6-fold) and caveolin (Cav1, 6-fold). In addition, cytokines/growth factors such as VEGF, TGF-β, FGF-23 and 11, interleukins (1α, 33 and 10), and PDGF gene expression is significantly increased in modelled μXg. Chemokines are chemotactic and modulate cellular functions in bone environment [Galliera et al., 2008]. Modelled μXg upregulated gene expression of chemokines such as CXCL4 (30-fold), CXCL14 (9.2-fold), CXCL2 (7.3-fold), CCL7 (16-fold), CCL8 (15-fold), CCL24 (4.7-fold) and CXCR4 (4-fold). Also, we identify that Ca^{2+} binding protein S100A8 was highly upregulated (72-fold) in modelled μXg, implicating a potential role of Ca^{2+} signalling in OCL activation under μXg conditions. Further, μXg significantly downregulated some negative regulators of OCL differentiation such as interleukin (IL)-12β (−7.7-fold), G-protein-coupled receptor (GPCR) 48 (−3.5-fold), estrogen receptor (ER)-β (−3.3-fold), P58 repressor (−2.2-fold) and interferon regulatory factor (IRF)-9 (−2.1-fold; Supplemental Table VIII). These results indicate that differential gene expression under μXg may have direct effect on OCL formation/function.

EVALUATION OF μXg-INDUCED GENE EXPRESSION DURING OCL DIFFERENTIATION

We confirmed the modelled μXg induced gene expression during OCL differentiation by real-time RT-PCR and Western blot analysis of mouse bone marrow cultures. As shown in Figure 3A, real-time RT-PCR analysis of total RNA isolated from bone marrow-derived non-adherent cells subjected to modelled μXg and stimulated with RANKL demonstrated a significant increase in the levels of MMP-8, MMP-12, MMP-13, CTS-L, CTS-B, CTS-K, CAR4, ATPase, S100A8, c-Jun and MITF mRNA expression compared to Xg cells. Western blot analysis of total cell lysates obtained from mouse bone marrow-derived preosteoclast cells revealed that Ctsk expression is significantly (2-fold) elevated under μXg compared to Xg cells (Fig. 3B). These results validate the microarray data and suggest modelled μXg stimulates cathepsins and MMPs expression in preosteoclast cells, which play an important role in matrix degradation/bone loss.

μXg MODULATION OF Ca^{2+}

RANKL signalling evokes Ca^{2+} oscillations during OCL differentiation [Takayanagi et al., 2002a]. Microarray analysis identified high-level expression of S100A8 (calcium-binding protein molecule A8/calgranulin A), a calcium-binding protein involved in the cell signal transduction and differentiation [Riau et al., 2009]. Interestingly, Western blot analysis of total cell lysates obtained from mouse bone marrow-derived non-adherent cells subjected to modelled μXg revealed induced expression (12-fold) of S100A8 in the presence or absence of RANKL stimulation (Fig. 3C). We then examined relative

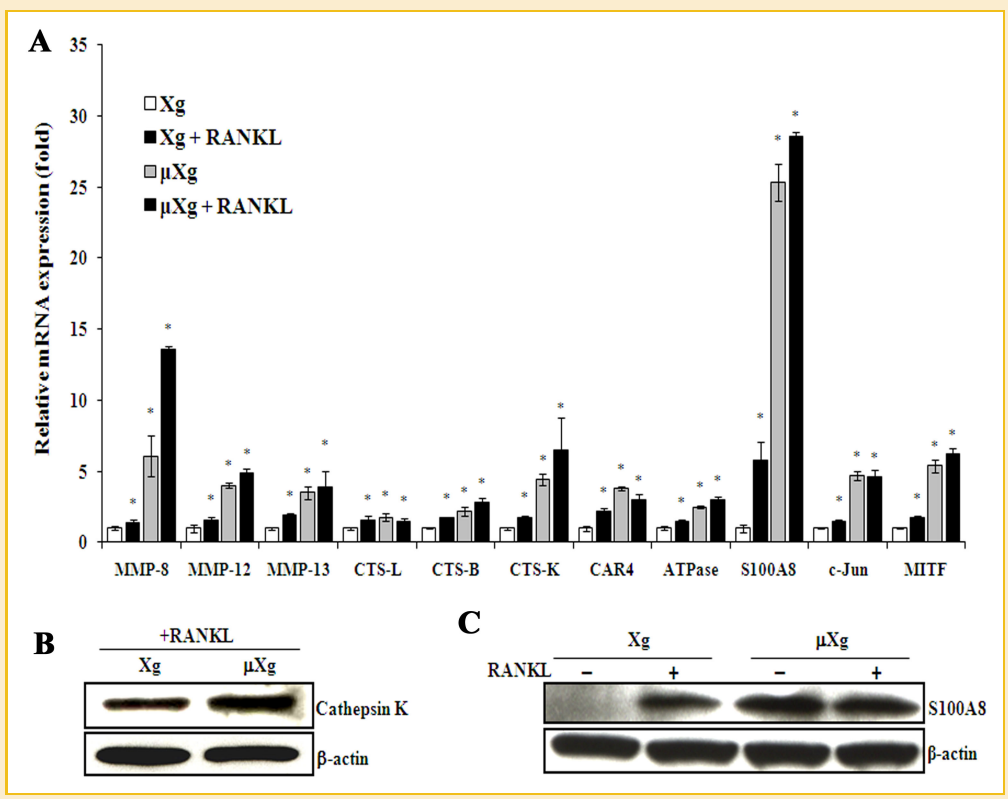

Fig. 3. Evaluation of μXg-induced gene expression by real-time RT-PCR and Western blot analysis. Mouse bone marrow-derived non-adherent cells were subjected to modelled μXg for 24 h or control (Xg) cells were stimulated with or without RANKL (80 ng/ml) for 24 h. A: Total RNA isolated was subjected to real-time RT-PCR using gene-specific primers as listed in Methods Section. The mRNA expression was normalized with respect to GAPDH amplification. Each bar represents the mean ± SD of three independent experiments ($^{*}P < 0.05$). B: Total cell lysates obtained were subjected to Western blot analysis using anti-cathepsin K and (C) anti-S100A8 antibodies. β-actin expression served as loading control.

changes in cytosolic calcium (Ca^{2+}) levels and oscillation patterns in RAW 264.7 cells subjected to modelled μXg. As shown in Figure 4A, modelled μXg elevated Ca^{2+} in these cells. Ca^{2+} changes were estimated as the ratio of fluorescence intensity of the Fluo-4 to Fura Red. Furthermore, Ca^{2+} oscillations were also elevated in RAW 264.7 cells subjected to modelled μXg compared to Xg cells (Fig. 4B). These results suggest that μXg elevated intracellular Ca^{2+} levels/oscillations which play important roles in OCL differentiation/activity. We further examined participation of S100A8 in μXg stimulated OCL differentiation. RAW 264.7 cells were transiently transfected with double-stranded siRNA against S100A8 using oligofectamine were subjected to modelled μXg for 24 h and cultured for 5 days to form multinucleated OCLs as described in Methods Section. As shown in Figure 4C, RAW 264.7 cells knockdown for S100A8 resulted in a significant decrease in OCL formation compared to scrambled non-specific siRNA transfected Xg cells. Ca^{2+} signalling activates calcineurin (CN) and calmodulin kinases (CaMKs) pathways which induce NFATc1 and CREB activation respectively, during OCL differentiation [Sato et al., 2006]. Therefore, we further determined NFATc1 and phospho-CREB (p-CREB) levels in RAW 264.7 cells subjected to modelled μXg. Western blot analysis of total cell lysates obtained from RAW 264.7 cells subjected to modelled μXg and stimulated with RANKL for 24 h period demonstrated no significant change in the levels of NFATc1 expression; however, a 5-fold increase in the levels of p-CREB compared to Xg (Fig. 4D,E). Taken together, these results implicate a functional role for S100A8 and elevated Ca^{2+} levels in μXg stimulated OCL differentiation.

DISCUSSION

Space flight is a challenge for normal bone homeostasis, and austronauts experience significant bone loss. Earlier, studies with the NASA developed RWV, RCCS revealed that modelled μXg stimulates osteoclastogenesis and bone resorption by increasing the RANKL/OPG ratio [Rucci et al., 2007]. Others have also reported that RCCS modelled μXg inhibits osteoblastogenesis and stimulates osteoclastogenesis [Saxena et al., 2007]. However, in studies using a 3D clinostat system to simulate μXg, inhibition of MC3T3-E1 cell differentiation and suppression of RANKL and OPG gene expression was observed. In addition, inhibition of fusion of RAW 264.7 cells to form multinucleated OCLs was reported, implicating long-term mechanical unloading and suppression of bone formation/resorption [Makihira et al., 2008]. More recently, in-flight studies conducted during the FOTON-3 mission revealed OCLs and their precursors as direct targets for μXg and that mechanical forces modulate genes associated with OCL differentiation/activity [Tamma et al., 2009]. Also, studies with mouse osteoblast cultures using the RWV bioreactor identified μXg regulated mechanoresponsive genes in osteoblasts [Patel et al., 2007; Capulli et al., 2009]. The present study confirms stimulation of osteoclastogenesis in modelled μXg using the RCCS. We further analyzed gene expression profile by Agilent microarray analysis during OCL differentiation of a homogeneous population of RAW 264.7 progenitor cells in a modelled μXg environment. Several genes important for osteoclastogenesis/bone resorption function are elevated under conditions of μXg compared to Xg cells. However, the differential gene expression in preosteoclast cells subjected to μXg and stimulated with RANKL for a short period (24 h) excludes the possibility due to differences in maturation of osteoclasts. Granulocyte colony-stimulating factor (G-CSF) has been shown to be a potent stimulator of OCL activity and inhibit osteoblasts activity [Hirbe et al., 2007; Horiuchi et al., 2009]. Therefore, μXg upregulated G-CSF expression may affect both OCL and osteoblast activity in the bone microenvironment. Furthermore, growth factors such as VEGF, TGF-β, FGF and PDGF play important roles in osteoclastogenesis [Zhang et al., 1998; Chikazu et al., 2000; Nakagawa et al., 2000; Fox et al., 2008]. TGF-β has multiple functions in the bone environment and is required for early OCL progenitor commitment and suppress OCL apoptosis [Janssens et al., 2005; Gingery et al., 2008]. Elevated TGF-β receptors I and II implicates a potential role in μXg-induced osteoclastogenesis.

Matrix metalloproteinases and cathepsins, cysteine protease expression in OCLs plays an important role in bone-resorption activity [Troen, 2004; Sundaram et al., 2007]. Microarray analysis revealed upregulation of cytokines/growth factors and several matrix-degrading proteases to suggest μXg modulation of OCL bone-resorption activity. Furthermore, elevated expression of integrins contributes to the OCL's localization and attachment to the bone surface [Lakkakorpi et al., 1991]. Modelled μXg upregulation of transcription factors, c-Jun, MITF and CREBs indicate μXg modulation of RANKL–RANK signalling critical for OCL differentiation. Likewise, Ctsk mRNA expression has been shown to be upregulated in OCL cultured in bioreactors that were subjected to space flight [Tamma et al., 2009] which support data from our microarray profile using RCCS modelled μXg. Our finding of elevated several growth factors in preosteoclast cells under μXg may alter RANKL and OPG levels in bone environment and facilitate enhanced OCL activity. We show modelled μXg elevated levels of cytosolic Ca^{2+} and calcium-binding protein S100A8 compared to Xg cells. The S100A8 molecule is associated with multiple targets that promote cell growth and differentiation, cell cycle regulation, gene transcription, cell surface receptor activities [Donato, 2001; Heizmann et al., 2002] and anti-apoptotic function [Lee et al., 2008]. Furthermore, our findings with high-level expression of S100A8 calcium-binding protein is associated with Ca^{2+} oscillations implicates an essential role in OCL differentiation under μXg conditions. We confirmed that S100A8 suppression in RAW 264.7 cells significantly decreased modelled μXg stimulated OCL differentiation. Ca^{2+} signalling through CN pathway induces NFATc1 transcription factor critical for OCL-specific gene expression such as cathepsins and MMPs [Takayanagi et al., 2002a; Sundaram et al., 2007; Balkan et al., 2009]. We find no significant change in the levels of NFATc1 expression, however increased levels of c-Jun, MITF and CREBs transcription factors in modelled μXg suggested that elevated Ca^{2+} oscillations modulates CaMK–CREB pathway during OCL differentiation. Accordingly, we identify elevated levels of p-CREB in preosteoclast cells subjected to modelled μXg compared to Xg gravity conditions. The CaMK–CREB pathway also regulates the expression of osteoclast-specific genes in cooperation with NFATc1 [Sato et al., 2006]. Previously,

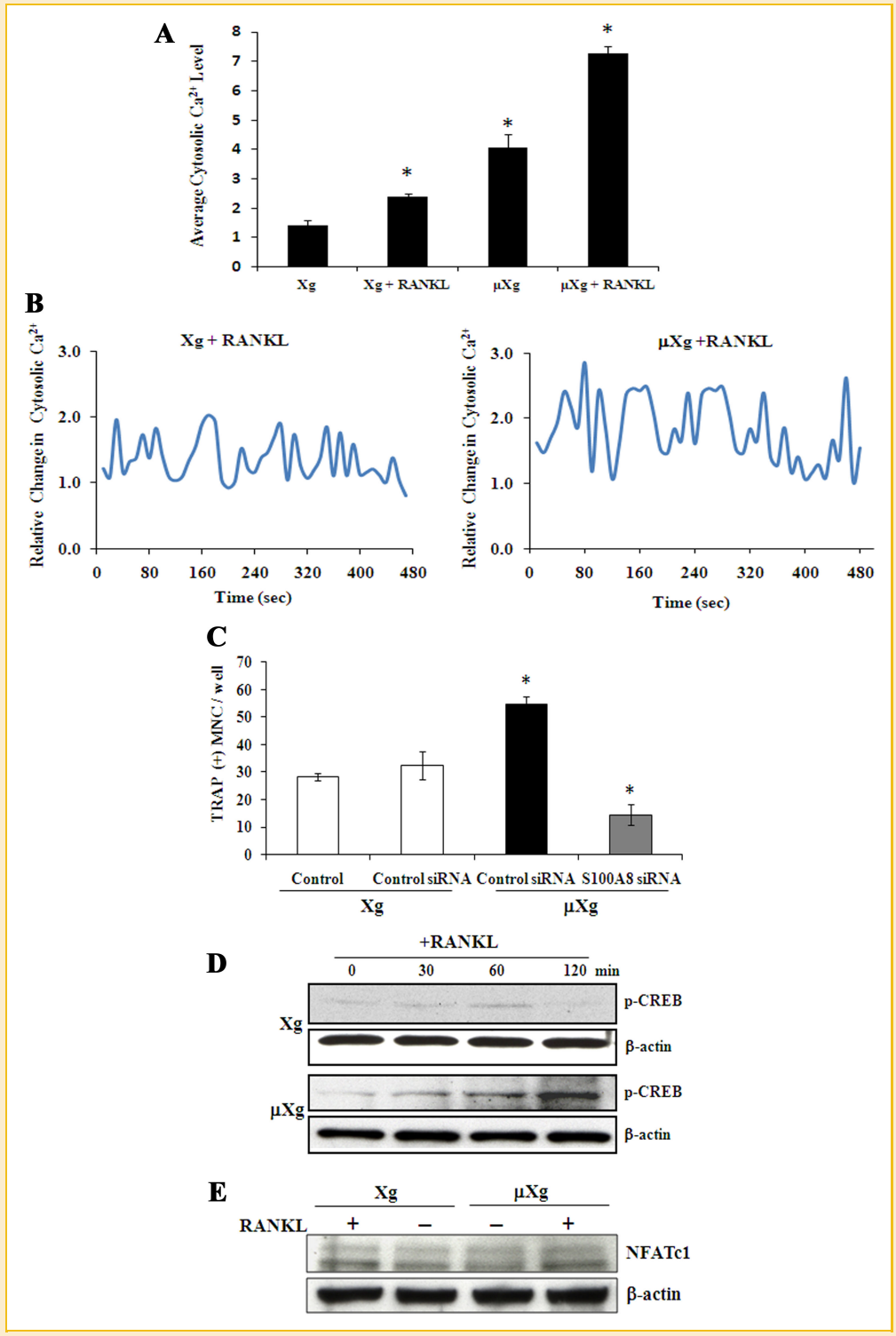

Fig. 4. Modelled μXg modulation of Ca^{2+} in RAW 264.7 cells. A: μXg modulates cytosolic Ca^{2+} levels in RAW 264.7 cells. Cells were incubated in the presence of fluo-4 AM (4.6 μM), and Fura Red AM (14 μM) and pluronic F127 (0.05%) for 30 min. Cells were post-incubated in IMDM medium without phenol red, 10% FBS, M-CSF (10 ng/ml) and RANKL (80 ng/ml) for 20 min and analyzed by a live-cell confocal microscope. The ratio of fluorescence intensity of Fluo-4 to Fura Red was calculated to estimate the intracellular calcium levels of the cells. Each bar represents the mean ± SD of three independent experiments ($^*P < 0.05$). B: μXg elevates Ca^{2+} oscillations in RAW 264.7 cells. Ca^{2+} oscillations were recorded in control (Xg) and modelled μXg subjected RAW 264.7 cells as the ratio of fluorescence intensity of the Fluo-4 to Fura Red plotted at 10 s intervals. The two fluorophores were equally distributed in cytosol and had identical ratios under saturating conditions. The fluorescence ratios were calculated using R_{min} and R_{max}. Results represent an average of 10 individual cells of three independent experiments. Pearson's correlation coefficient of the two groups, Xg ($R^2 = 0.29$) and μXg ($R^2 = 0.55$) were calculated. C: S100A8 regulates osteoclastogenesis in modelled μXg. RAW 264.7 cells were transiently transfected with double-stranded S100A8 siRNA using oligofectamine. Cells were subjected to either modelled μXg for 24 h or Xg and stimulated with RANKL (80 ng/ml) for 5 days. TRAP-positive multinucleated cells (MNC) containing three or more nuclei were scored as OCL. The results represent quadruplicate cultures of three independent experiments ($^*P < 0.05$). D: Modelled μXg elevates phospho-CREB (p-CREB) levels in RAW 264.7 cells. Total cell lysates obtained from RAW 264.7 cells subjected to modelled μXg or Xg and stimulated with RANKL (80 ng/ml) for indicated period (0–120 min) were analyzed by Western blot using anti-p-CREB specific antibody. E: NFATc1 expression in RAW 264.7 cells. Total cell lysates obtained from RAW 264.7 cells subjected to modelled μXg or Xg and stimulated with or without RANKL (80 ng/ml) for 24 h were analyzed for NFATc1 expression using anti-NFATc1 antibody. β-actin expression in all the samples analyzed served as loading control. [Color figure can be viewed in the online issue, which is available at wileyonlinelibrary.com]

CaMK–CREB dependent c-Jun activation by calcium signalling has been demonstrated [Cruzalegui et al., 1999]. Furthermore, downregulation of negative regulators of osteoclastogenesis such as IL-12β, IL-13, GPCR 48, IFN-β downstream signalling molecules such as P58 repressor and IRF-9 implicates a potential role in OCL differentiation/activity under μXg conditions [Hayashi et al., 2002; Takayanagi et al., 2002b; Luo et al., 2009]. Collectively, our results suggest that modelled μXg modulates OCL development/function. In summary, modelled μXg regulated gene expression profiling in preosteoclast cells provide new insights into molecular mechanisms and therapeutic targets of OCL differentiation/activation to prevent bone loss and fracture risk in astronauts during space flight missions.

ACKNOWLEDGMENTS

We greatly appreciate Dr. Ruth K. Globus at NASA Ames Research Center for help to establish the RWV, RCCS in our laboratory. We thank Dr. W. Scott Argraves and Dr. Jeremy L. Barth, for coordinating undergraduate student summer research training program (SURP) at the Medical University of South Carolina.

REFERENCES

Arbeille P, Fomina G, Pottier JM, Achaibou F, Kotovskaya A. 1995. Influence of the thigh cuffs countermeasure on the cardiovascular adaptation to 0.g (14 and 21 day Mir spaceflights). J Gravit Physiol 2:P9–P10.

Balkan W, Martinez AF, Fernandez I, Rodriguez MA, Pang M, Troen BR. 2009. Identification of NFAT binding sites that mediate stimulation of cathepsin K promoter activity by RANK ligand. Gene 446:90–98.

Berezovska OP, Rodionova NV, Grigoryan EN, Mitashov VI. 1998. Changes in the numbers of osteoclasts in newts under conditions of microgravity. Adv Space Res 21:1059–1063.

Bustin SA. 2000. Absolute quantification of mRNA using real-time reverse transcription polymerase chain reaction assays. J Mol Endocrinol 25:169–193.

Capulli M, Rufo A, Teti A, Rucci N. 2009. Global transcriptome analysis in mouse calvarial osteoblasts highlights sets of genes regulated by modeled microgravity and identifies a ''mechanoresponsive osteoblast gene signature''. J Cell Biochem 107:240–252.

Carmeliet G, Bouillon R. 1999. The effect of microgravity on morphology and gene expression of osteoblasts in vitro. FASEB J 13(Suppl):S129–S134.

Cavanagh PR, Licata AA, Rice AJ. 2005. Exercise and pharmacological countermeasures for bone loss during long-duration space flight. Gravit Space Biol Bull 18:39–58.

Chikazu D, Hakeda Y, Ogata N, Nemoto K, Itabashi A, Takato T, Kumegawa M, Nakamura K, Kawaguchi H. 2000. Fibroblast growth factor (FGF)-2 directly stimulates mature osteoclast function through activation of FGF receptor 1 and p42/p44 MAP kinase. J Biol Chem 275:31444–31450.

Cruzalegui FH, Hardingham GE, Bading H. 1999. c-Jun functions as a calcium-regulated transcriptional activator in the absence of JNK/SAPK1 activation. EMBO J 18:1335–1344.

Donato R. 2001. S100: A multigenic family of calcium-modulated proteins of the EF-hand type with intracellular and extracellular functional roles. Int J Biochem Cell Biol 33:637–668.

Fox SW, Evans KE, Lovibond AC. 2008. Transforming growth factor-beta enables NFATc1 expression during osteoclastogenesis. Biochem Biophys Res Commun 366:123–128.

Galliera E, Locati M, Mantovani A, Corsi MM. 2008. Chemokines and bone remodeling. Int J Immunopathol Pharmacol 21:485–491.

Garber MA, McDowell DL, Hutton WC. 2000. Bone loss during simulated weightlessness: A biomechanical and mineralization study in the rat model. Aviat Space Environ Med 71:586–592.

Gingery A, Bradley EW, Pederson L, Ruan M, Horwood NJ, Oursler MJ. 2008. TGF-beta coordinately activates TAK1/MEK/AKT/NFkB and SMAD pathways to promote osteoclast survival. Exp Cell Res 314:2725–2738.

Goodwin TJ, Schroeder WF, Wolf DA, Moyer MP. 1993. Rotating-wall vessel coculture of small intestine as a prelude to tissue modeling: Aspects of simulated microgravity. Proc Soc Exp Biol Med 202:181–192.

Hayashi T, Kaneda T, Toyama Y, Kumegawa M, Hakeda Y. 2002. Regulation of receptor activator of NF-kappa B ligand-induced osteoclastogenesis by endogenous interferon-beta (INF-beta) and suppressors of cytokine signaling (SOCS). The possible counteracting role of SOCSs- in IFN-beta-inhibited osteoclast formation. J Biol Chem 277:27880–27886.

Heizmann CW, Fritz G, Schafer BW. 2002. S100 proteins: Structure, functions and pathology. Front Biosci 7:d1356–d1368.

Hirbe AC, Uluckan O, Morgan EA, Eagleton MC, Prior JL, Piwnica-Worms D, Trinkaus K, Apicelli A, Weilbaecher K. 2007. Granulocyte colony-stimulating factor enhances bone tumor growth in mice in an osteoclast-dependent manner. Blood 109:3424–3431.

Horiuchi K, Kimura T, Miyamoto T, Miyamoto K, Akiyama H, Takaishi H, Morioka H, Nakamura T, Okada Y, Blobel CP, Toyama Y. 2009. Conditional inactivation of TACE by a Sox9 promoter leads to osteoporosis and increased granulopoiesis via dysregulation of IL-17 and G-CSF. J Immunol 182:2093–2101.

Hughes-Fulford M, Lewis ML. 1996. Effects of microgravity on osteoblast growth activation. Exp Cell Res 224:103–109.

Janssens K, ten Dijke P, Janssens S, Van Hul W. 2005. Transforming growth factor-beta1 to the bone. Endocr Rev 26:743–774.

Kanematsu M, Yoshimura K, Takaoki M, Sato A. 2002. Vector-averaged gravity regulates gene expression of receptor activator of NF-kappaB (RANK) ligand and osteoprotegerin in bone marrow stromal cells via cyclic AMP/protein kinase A pathway. Bone 30:553–558.

Katkovsky BS, Pomyotov YD. 1976. Cardiac output during physical exercises following real and simulated space flight. Life Sci Space Res 14:301–305.

Keyak JH, Koyama AK, LeBlanc A, Lu Y, Lang TF. 2009. Reduction in proximal femoral strength due to long-duration spaceflight. Bone 44: 449–453.

Lakkakorpi PT, Horton MA, Helfrich MH, Karhukorpi EK, Vaananen HK. 1991. Vitronectin receptor has a role in bone resorption but does not mediate tight sealing zone attachment of osteoclasts to the bone surface. J Cell Biol 115:1179–1186.

Lang T, LeBlanc A, Evans H, Lu Y, Genant H, Yu A. 2004. Cortical and trabecular bone mineral loss from the spine and hip in long-duration spaceflight. J Bone Miner Res 19:1006–1012.

Lang TF, Leblanc AD, Evans HJ, Lu Y. 2006. Adaptation of the proximal femur to skeletal reloading after long-duration spaceflight. J Bone Miner Res 21:1224–1230.

Lee YS, Sohn KC, Jang S, Lee Y, Hwang C, Kim KH, Cho MJ, Kim CD, Lee JH. 2008. Anti-apoptotic role of S100A8 in X-ray irradiated keratinocytes. J Dermatol Sci 51:11–18.

Luo J, Zhou W, Zhou X, Li D, Weng J, Yi Z, Cho SG, Li C, Yi T, Wu X, Li XY, de Crombrugghe B, Hook M, Liu M. 2009. Regulation of bone formation and remodeling by G-protein-coupled receptor 48. Development 136:2747–2756.

Makihira S, Kawahara Y, Yuge L, Mine Y, Nikawa H. 2008. Impact of the microgravity environment in a 3-dimensional clinostat on osteoblast- and osteoclast-like cells. Cell Biol Int 32:1176–1181.

Miyamoto A, Shigematsu T, Fukunaga T, Kawakami K, Mukai C, Sekiguchi C. 1998. Medical baseline data collection on bone and muscle change with space flight. Bone 22:79S–82S.

Nakagawa M, Kaneda T, Arakawa T, Morita S, Sato T, Yomada T, Hanada K, Kumegawa M, Hakeda Y. 2000. Vascular endothelial growth factor (VEGF) directly enhances osteoclastic bone resorption and survival of mature osteoclasts. FEBS Lett 473:161–164.

Nemoto A, Uemura T. 2000. Hypergravity effects on osteoclasts activity. J Gravit Physiol 7:P127–P128.

Nichols HL, Zhang N, Wen X. 2006. Proteomics and genomics of microgravity. Physiol Genomics 26:163–171.

Patel MJ, Liu W, Sykes MC, Ward NE, Risin SA, Risin D, Jo H. 2007. Identification of mechanosensitive genes in osteoblasts by comparative microarray studies using the rotating wall vessel and the random positioning machine. J Cell Biochem 101:587–599.

Reddy SV. 2004. Regulatory mechanisms operative in osteoclasts. Crit Rev Eukaryot Gene Expr 14:255–270.

Riau AK, Wong TT, Beuerman RW, Tong L. 2009. Calcium-binding S100 protein expression in pterygium. Mol Vis 15:335–342.

Rucci N, Migliaccio S, Zani BM, Taranta A, Teti A. 2002. Characterization of the osteoblast-like cell phenotype under microgravity conditions in the NASA-approved rotating wall vessel bioreactor (RWV). J Cell Biochem 85:167–179.

Rucci N, Rufo A, Alamanou M, Teti A. 2007. Modeled microgravity stimulates osteoclastogenesis and bone resorption by increasing osteoblast RANKL/OPG ratio. J Cell Biochem 100:464–473.

Sato K, Suematsu A, Nakashima T, Takemoto-Kimura S, Aoki K, Morishita Y, Asahara H, Ohya K, Yamaguchi A, Takai T, Kodama T, Chatila TA, Bito H, Takayanagi H. 2006. Regulation of osteoclast differentiation and function by the CaMK–CREB pathway. Nat Med 12:1410–1416.

Saxena R, Pan G, McDonald JM. 2007. Osteoblast and osteoclast differentiation in modeled microgravity. Ann NY Acad Sci 1116:494–498.

Shanmugarajan S, Irie K, Musselwhite C, Key LL, Jr., Ries WL, Reddy SV. 2007. Transgenic mice with OIP-1/hSca overexpression targeted to the osteoclast lineage develop an osteopetrosis bone phenotype. J Pathol 213: 420–428.

Sonnenfeld G, Butel JS, Shearer WT. 2003. Effects of the space flight environment on the immune system. Rev Environ Health 18:1–17.

Sundaram K, Nishimura R, Senn J, Youssef RF, London SD, Reddy SV. 2007. RANK ligand signaling modulates the matrix metalloproteinase-9 gene expression during osteoclast differentiation. Exp Cell Res 313:168–178.

Takayanagi H, Kim S, Koga T, Nishina H, Isshiki M, Yoshida H, Saiura A, Isobe M, Yokochi T, Inoue J, Wagner EF, Mak TW, Kodama T, Taniguchi T. 2002a. Induction and activation of the transcription factor NFATc1 (NFAT2) integrate RANKL signaling in terminal differentiation of osteoclasts. Dev Cell 3:889–901.

Takayanagi H, Kim S, Taniguchi T. 2002b. Signaling crosstalk between RANKL and interferons in osteoclast differentiation. Arthritis Res 4(Suppl 3):S227–S232.

Tamma R, Colaianni G, Camerino C, Di Benedetto A, Greco G, Strippoli M, Vergari R, Grano A, Mancini L, Mori G, Colucci S, Grano M, Zallone A. 2009. Microgravity during spaceflight directly affects in vitro osteoclastogenesis and bone resorption. FASEB J 23:2549–2554.

Troen BR. 2004. The role of cathepsin K in normal bone resorption. Drug News Perspect 17:19–28.

Van Loon JJ, Bervoets DJ, Burger EH, Dieudonne SC, Hagen JW, Semeins CM, Doulabi BZ, Veldhuijzen JP. 1995. Decreased mineralization and increased calcium release in isolated fetal mouse long bones under near weightlessness. J Bone Miner Res 10:550–557.

White RJ, Blomqvist CG. 1998. Central venous pressure and cardiac function during spaceflight. J Appl Physiol 85:738–746.

Zayzafoon M, Gathings WE, McDonald JM. 2004. Modeled microgravity inhibits osteogenic differentiation of human mesenchymal stem cells and increases adipogenesis. Endocrinology 145:2421–2432.

Zhang Z, Chen J, Jin D. 1998. Platelet-derived growth factor (PDGF)-BB stimulates osteoclastic bone resorption directly: The role of receptor beta. Biochem Biophys Res Commun 251:190–194.

Zhang B, Schmoyer D, Kirov S, Snoddy J. 2004. GOTree Machine (GOTM): A web-based platform for interpreting sets of interesting genes using Gene Ontology hierarchies. BMC Bioinformatics 5:16.